Preface

The idea of creating a book of this genre came with the realization that there were no books in the open literature that combined the materials aspect of piezoelectric and acoustic materials together with the principles of transducer design and recent advances in piezoelectric transducers, as well as their application. By combining topics such as Fundamentals of Piezoelectricity (Part I), Piezoelectric and Acoustic Materials for Transducer Technology (Part II), Transducer Design Principles (Part III), and Piezoelectric Transducer Fabrication Methods (Part IV), our purpose was to provide a comprehensive and self-consistent volume whereby the aforementioned lack of a reference book in the open literature can be remedied.

This book is comprised of four complementary sections. In Part I, a concise treatment of piezoelectric phenomena in solids is presented. Chapter 1 by Akdoğan and Safari establishes the solid-state thermodynamic foundation for ferroelectricity as all piezoelectrics used in today's transducer technology are ferroelectric. It also delineates the origin of very important concepts such as spontaneous polarization, hysteresis loops, and piezostrain coefficients, which are needed to describe the macroscopic behavior of piezoelectrics. The chapter by Kholkin, Pertsev, and Goltsev (Chap. 2) deals with the symmetry aspects of the piezoelectric effect in various materials (single crystals, ceramics, and thin films). It defines the third-rank tensor of piezoelectric coefficients in reference to the fundamentals of crystallography, and then discusses the orientation dependence of the longitudinal piezoelectric response in ferroelectric single crystals. Also, a concise discussion on the effective piezoelectric constants of polydomain crystals, ceramics, and thin films and their dependence on crystal symmetry is provided. The domain-wall contribution to the piezoelectric properties of ferroelectric ceramics and thin films is also given. Finally, the crystallographic principles of piezomagnetic, magnetoelectric, and multiferroic materials are presented. In Chap. 3, Trolier-McKinstry presents a detailed description of the crystallochemical principles of ferroelectricity and piezoelectricity in solids. The discussion covers perovskites, tolerance factors, domains and domain walls, the lead zirconate titanate (PZT) system, bismuth-layer

structure, $LiNbO_3$, tungsten bronze structure, and SbSI, which is the point of departure in the development of piezoelectric composites. The emphasis is on the atomic arrangements leading to polarization and its consequences on material properties.

In Part II, three chapters are devoted to the most prominent piezoelectric and acoustic material systems currently either in use or in development for transducer applications. Damjanovic (Chap. 4) gives a detailed account on lead-based ferroelectrics/piezoelectrics, including $PbTiO_3$, PZT, relaxor ferroelectrics, and single crystals. Therein, one could find an in-depth discussion of the morphotrophic phase boundary in the PZT system as well as the anisotropy in piezoelectric response in $PbTiO_3$. Systems with compositional modifications are treated as well, where hard and soft ferroelectrics are introduced. Kosec et al. (Chap. 5) gives a full overview of the (K, Na)NbO_3 system, which is the most important lead-free ferroelectric system whose compositional modifications have great promise for applications in the future. The emphasis is on the processing of ceramics such as $KNbO_3$, $NaNbO_3$, (K, Na)NbO_3, and the recently discovered KNN–LT–LS ternary system, thereby effectively establishing processing-property relations. Also, a wealth of material properties appertaining to the (K, Na)NbO_3 and related systems are included therein. Chap. 6 by Takenaka is on bismuth-based ferroelectric ceramics, which is another lead-free system of utmost importance. The major focus there is on the $Bi_4Ti_3O_{12}$ and its compositional modifications. Most importantly, Takenaka provides a very thorough treatment of grain orientation (texturing) of such lead-free ceramics, and discusses its consequences on piezoelectric properties. Cheng et al. (Chap. 7) presents a very detailed overview of the advances in electromechanically active polymers in the context of mechatronics and artificial muscle. After a concise review of the appertaining phenomenology on electromechanical behavior in solids, he and his colleagues present systems such as PVDF, P(VDF–TrFE) copolymer, and terpolymers. A very comprehensive discussion on phase transitions, structure, and electromechanical response is provided along with sets of material properties. In Chap. 8, Yamashita et al. introduce the recent advances in acoustic lens materials and provide a systematic account on recent advances in silicon-based technologies. Therein, the evolution of acoustic properties of silicon lenses are discussed from the processing vantage point, and the most prominent dopants for composite-making are identified. Part II ends with another chapter on acoustic lens materials by Kondo, which summarizes the use of carbon fiber composites and how a wide range of acoustic impedances can be fashioned for transducer applications.

Part III is devoted to transducer design principles. First, Lethiecq et al. (Chap. 10) discuss the design principles governing medical ultrasound transducers. The performance metrics of such transducers are introduced, operation principles of single element and transducer arrays are elaborated on, and the underlying acoustic principles are discussed. In Chap. 11, Tressler discusses the design principles of transducers for sonar applications. Various in-air and under-water calibration techniques are first presented, followed by various projector designs (ring, bender bar, flexural disks, flextensional, tonpilz) are introduced and appertaining design methodologies are elaborated on. Also included in that chapter are hydrophone design principles, including cylinder and sphere configurations. This section ends

with Chap. 12, where Hladky-Hennion provides a comprehensive overview of finite element modeling (FEM) principles as applied to piezoelelectric transducers. First, the mathematical foundations are provided through constitutive equations, the variational principle, and appertaining functionals. Then, the application of the FEM method is demonstrated. Analysis methods such as static, harmonic, modal, and transient are given. The chapter concludes with examples on the analysis of cymbal transducers and cymbal arrays, and 1–3 composite transducers.

Part IV is on transducer fabrication methods. Therefore, it is inherently tied into applications as well since fabrication methods tend to be application specific. In Chap. 13, Schoenecker addresses the status of piezoelectric fiber composite fabrication, and focuses on three topics: the preparation of sol–gel-derived PZT fiber/polymer composites, the soft-mold method with high achievement potential for preparing tailor-made composites and understanding the structure–property relationships, and the preparation of powder suspension-derived PZT fiber/polymer composites as the technologically advanced and commercialized process. Therein, it is iterated that the use of piezoceramic fibers allows for the fabrication of high-quality fiber composites, surpassing performance metrics that cannot be achieved by the conventional dice and fill technique. Beige and Steinhausen (Chap. 14) discuss different types of composition gradient systems for bending actuators. The combination of hard and soft piezoelectric ceramics and electrostrictive and electroconductive materials are introduced. Processing strategies are summarized and a mathematical models for modeling of poling in such combined systems are presented. The results of theoretical analysis are compared with experimental data for lead-free systems based on barium titanate. In Chap. 15, Smay et al. present the advances made in the use of robocasting solid freeform fabrication (SFF) technique based on the direct writing of highly concentrated colloidal gels. They show that robocasting offers facile assembly of complex three-dimensional geometries and a broad pallet of ceramic, metallic, and polymeric materials from which devices can be developed. Examples of PZT skeletons for direct use or to create epoxy-filled composites suitable for hydrostatic piezoelectric sensors are given. PZT composites of (3–3, 3–2, 3–1) connectivity are demonstrated. It is shown that the figure of merit $(d_h g_h)$ increases by up to 60-fold compared with bulk PZT in such composites. In Chap. 16, Jantunen et al. present a comprehensive overview of the general properties and requirements of piezoelectric micropositioners. Special attention is paid to stiffness related to other actuator properties, with general rules and examples. Also the control and sensor techniques required to avoid or minimize the nonlinearities of the piezoelectric device are discussed in detail. And it is shown that in micropositioning a profound overall know–how about material properties, actuator design, and control, sensor and driving techniques are required in addition to an in-depth knowledge of application requirements. Finally, some commercial applications utilizing piezoelectric micropositioners are given as examples. Doğan and Uzgur (Chap. 17) present a broad review of the application of piezoelectric transducers. Piezoelectric actuators are compared with magnetically active and thermally active actuators, and then piezoelectric actuators and their design and fabrication, especially traditional piezoelectric transducers with newly designed flextensional transducers, are compared.

Finally, application-related issues are discussed on Chap. 18 by Shashank et al. provides strategies for the selection of the piezoelectric transducers based on the frequency and amplitude of the mechanical stress in the context of energy harvesting. The figure of merit for the material selection is shown to be directly proportional to the product $(d \times g)$. The criterion for maximization of the product is discussed in depth, and results are reported on various devices utilizing piezoelectric bimorph transducers. Or and Chan (Chap. 19) present recent advances in piezocomposite ultrasonic transducers for high-frequency wire bonding of semiconductor packages. The principles of wire-bonding and appertaining challenges are summarized. The use of 1–3 piezocomposite rings in such applications is shown, and the electromechanical characteristics are presented. The chapter also includes a section on the evaluation of wire-bonding performance utilizing such transducers. Bassiri-Gharb (Chap. 20) presents the use of piezoelectrics in MEMS applications. In that chapter, the properties of AlN, ZnO, PZT, and PMN–PT films are reviewed, and the effect of substrate clamping is briefly discussed. Then fabrication and integration issues are addressed. Various applications of piezoelectrics, including AFM probe tips, RF switches, micromirrors, micropumps, and microvalves are given. In Chap. 21, Shung et al. discuss high-frequency ultrasonic transducers and arrays. After a thorough overview of the state of the art, $LiNbO_3$ single-crystal transducers, and PMN–PT single-crystal needle transducers for Doppler flow measurements are presented. A multitude of transducer designs are shown (annular arrays, linear arrays, and their derivatives), and underlying processing issues are elaborated on. The last chapter of the section and the book is on micromachining of piezoelectric transducers by Pappalardo et al. (Chap. 22). The basic principles, the fabrication processes, and some modeling approaches of novel micromachined ultrasonic transducers (MUTs) are described. It is shown that these transducers utilize the flextensional vibration of an array of micro-membranes called cMUT (capacitive MUT). It is also shown that good echographic images of internal organs in the human body have been obtained, demonstrating the possibilities of this technology to be utilized in commercial 1D and 2D probes for medical applications.

In conclusion, we thank all the contributing authors for their great zeal and industry in composing their respective chapters. Were it not for their willingness to participate in this exciting project, none that was accomplished could have been possible. A project of this magnitude cannot see the light of day without a constant source of encouragement and support. To that end, we express our gratefulness to our families, friends, and colleagues. Last but not the least, we thank Springer for giving us great flexibility in regard to the size of this volume.

Piscataway, New Jersey

A. Safari
E.K. Akdoğan

Chapter 2
Piezoelectricity and Crystal Symmetry

A.L. Kholkin,* N.A. Pertsev, and A.V. Goltsev

In this chapter, the symmetry aspects of the piezoelectric effect in various materials (single crystals, ceramics, and thin films) are briefly overviewed. First, the third-rank tensor of piezoelectric coefficients defined in the crystallographic reference frame is discussed. On this basis, the orientation dependence of the longitudinal piezoelectric response in ferroelectric single crystals is described. This dependence is especially important for relaxor single crystals, where a giant piezoelectric effect is observed. Then, the effective piezoelectric constants of polydomain crystals, ceramics, and thin films and their dependence on crystal symmetry are discussed. The domain-wall contribution to the piezoelectric properties of ferroelectric ceramics and thin films is also described. Finally, the crystallographic principles of piezomagnetic, magnetoelectric, and multiferroic materials are presented.

2.1 Historical Overview

Piezoelectricity (or, following direct translation from Greek word *piezein*, "pressure electricity") was discovered by Jacques Curie and Pierre Curie as early as in 1880 (Curie and Curie 1880). By analogy with temperature-induced charges in pyroelectric crystals, they observed electrification under mechanical pressure of certain crystals, including tourmaline, quartz, topaz, cane sugar, and Rochelle salt. This effect was distinguished from other similar phenomena such as "contact electricity" (friction-generated static charge). Even at this stage, it was clearly understood that symmetry plays a decisive role in the piezoelectric effect, as it was observed only for

A.L. Kholkin
Center for Research in Ceramics and Composite Materials (CICECO) & Department of Ceramics and Glass Engineering, University of Aveiro, 3810-193 Aveiro, Portugal
and
A. F. Ioffe Physico-Technical Institute of the Russian Academy of Sciences, 194021 St. Petersburg, Russia

A. Safari, E.K. Akdoğan (eds.) *Piezoelectric and Acoustic Materials for Transducer Applications*.

certain crystal cuts and mostly in pyroelectric materials in the direction normal to polar axis. However, Curie brothers could not predict a converse piezoelectric effect, i.e., deformation or stress under applied electric field. This important property was then mathematically deduced from the fundamental thermodynamic principles by Lippmann (1881). The existence of the converse effect was immediately confirmed by Curie brothers in the following publication (Curie and Curie 1881). Since then, the term *piezoelectricity* is commonly used for more than a century to describe the ability of materials to develop electric displacement **D** that is directly proportional to an applied mechanical stress σ (Fig. 2.1a). Following this definition, the electric charge appeared on the electrodes reverses its sign if the stress is changed from tensile to compressive. As follows from thermodynamics, all piezoelectric materials are also subject to a converse piezoelectric effect (Fig. 2.1b), i.e., they deform under applied electric field. Again, the sign of the strain **S** (elongation or contraction) changes to the opposite one if the direction of electric field **E** is reversed. Shear piezoelectric effect (Fig. 2.1c) is also possible, as it linearly couples shear mechanical stress or strain with the electric charge.

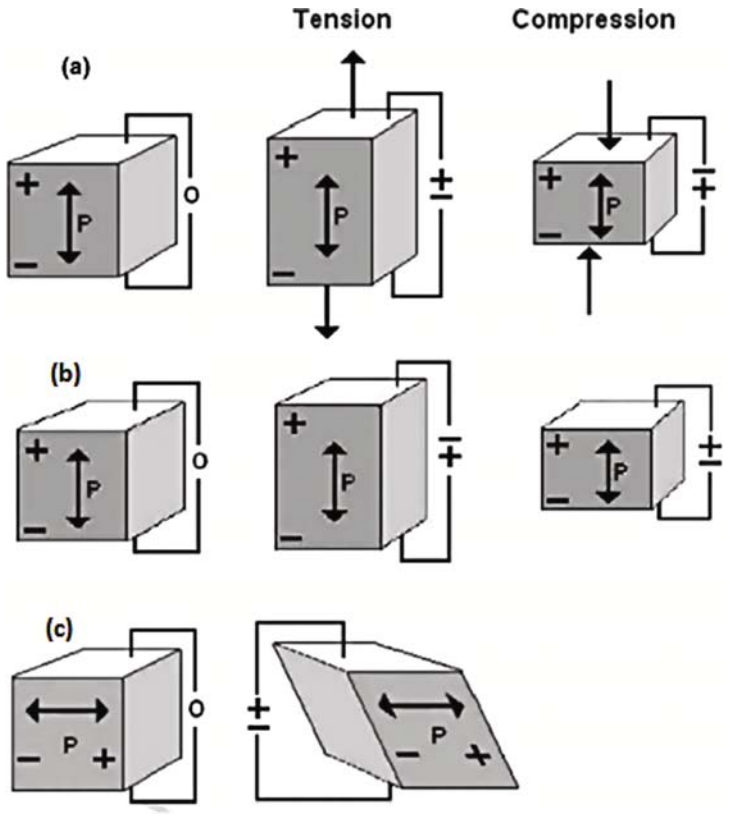

Fig. 2.1 Schematic representation of the longitudinal direct (**a**), converse (**b**), and shear (**c**) piezoelectric effects

Just after the discovery of piezoelectricity, much more work has been done to define crystallographic principles of the effect. In 1910, Voigt published the first textbook on physical crystallography (Voigt 1910), in which the correct description of the piezoelectric effect in different crystallographic classes was given. However, at that time the phenomenon of piezoelectricity was obscure because of a complicated description in crystals with low symmetry and no visible applications. Only after the Second World War the piezoelectric effect evolved from just a laboratory curiosity to a multimillion dollar industry with applications ranging from underwater sonars and medical imaging systems to car accelerometers. This was mainly due to the invention of piezoelectric ceramics (see, e.g., the textbook by Jaffe, Cook, and Jaffe (Jaffe et al. 1971)), in which the averaging of piezoelectric responses of individual crystallites (grains) in $PbZrO_3$–$PbTiO_3$ (PZT) solid solutions resulted in the high-symmetry ($\infty\infty m$) macroscopic state with only few independent piezoelectric coefficients of sufficiently high values. This research has resulted in the astonishing performance of piezoelectric materials with industrial applications in many areas. Currently, there is an immense interest in the materials with giant piezoelectric effect, so-called relaxor single crystals (Park and Shrout 1997), where the high piezoelectric activity is partly due to their symmetry.

2.2 Fundamentals of the Piezoelectric Effect in Single Crystals and Ceramics

Since the piezoelectric coupling is described by a linear relationship between the first-rank tensor or vector (**D** or **E**) and the second-rank tensor (σ or **S**), the corresponding coupling coefficients d_{kij} (also called charge piezoelectric coefficients) form a third-rank tensor. Hence, the piezoelectric equations may be written in the following form ($i,\ j,\ k = 1,\ 2,\ 3$):

$$S_{ij} = d_{kij}E_k, \tag{2.1}$$

$$D_k = d_{kij}\sigma_{ij}, \tag{2.2}$$

where the Einstein's summation rule for repeated indices is implied. Both direct and converse piezoelectric effects are frequently expressed using the reduced matrix notation d_{km}, where k denotes the component of electric displacement **D** or field **E** in the Cartesian reference frame ($x_1,\ x_2,\ x_3$), and the index $m = 1,\ldots,6$ is used to define the mechanical stress or strain. In this case, $m = 1$, 2, and 3 correspond to the normal stresses along the $x_1,\ x_2$, and x_3 axes, respectively, whereas $m = 4$, 5, and 6 denote the shear stresses $S_{23},\ S_{13}$, and S_{12}.

As mentioned earlier, it was understood from the very beginning that the crystallographic symmetry of materials plays a decisive role in the piezoelectric phenomena. According to the definition of the piezoelectric effect, all components of the piezoelectric tensor should vanish in crystals possessing the center of symmetry.

In the remaining 21 noncentrosymmetric crystallographic classes, the piezoelectricity may exist, except for the cubic class 432, where the piezoelectric charges developed along the $\langle 111 \rangle$ polar axes cancel each other. However, the absence of piezoelectricity in this particular case does not play any significant role, because there are only few crystals that belong to this class. In this context, it should be mentioned that statistically about 30% of all materials (from about several millions known by now) are noncentrosymmetric. However, the piezoelectric properties are revealed in only few thousands of them, with about several hundreds having piezoelectric activity valuable for the applications. Therefore, it can be concluded that the absence of the center of symmetry represents the necessary but not sufficient requirement for a material to exhibit any sizeable piezoelectric effect. Though the symmetry does not determine the values of piezoelectric coefficients directly, the symmetry considerations, as it will be shown in the next sections, are indispensable for the design and fabrication of piezoelectric and acoustic devices. Table 2.1 lists the point groups that permit piezoelectricity for all crystallographic systems.

The number N of independent components of a third-rank tensor, in principle, may be as large as $3^3 = 27$. The piezoelectric tensor, however, can have maximum of 18 independent components because $d_{kij} = d_{kji}$ owing to the symmetry of the stress and strain tensors ($\sigma_{ij} = \sigma_{ji}$; $S_{ij} = S_{ji}$). The case of $N = 18$ corresponds to triclinic crystals of class 1. In crystals with higher symmetry, the number N reduces further. This feature follows from the Neumann's principle: The symmetry elements of any physical property of a crystal must include the symmetry elements of the point group of this crystal. As a result, in tetragonal crystals of the 4*mm* symmetry, for example, there are only three independent components, and the piezoelectric effect is described by the matrix shown in Fig. 2.2.

Among the 20 piezoelectric crystal classes, there are ten *pyroelectric* point groups that possess a unique polar axis. Pyroelectric crystals contain a built-in polarization, which manifests itself in temperature-induced changes of the total

Table 2.1 Centrosymmetric and noncentrosymmetric point groups in crystals with different symmetries

Crystal system	Symmetry elements	Centro-symmetric	Noncentro-symmetric
Triclinic	Center	$\underline{1}$	1
Monoclinic	Center, axis, plane	$2/m$	2, m
Orthorhombic	Center, axis, plane	mmm	222, $mm2$
Tetragonal	Center, axis, plane	$4/m$, $4/mmm$	4, $\underline{4}$, 422, 4mm, $\underline{4}2m$
Trigonal	Center, axis, plane	$\underline{3}$, $\underline{3}m$	3, 32, 3m
Hexagonal	Center, axis, plane	$6/m$, $6/mmm$	6, $\underline{6}$, 622, 6mm, $\underline{6}m2$
Cubic	Center, axis, plane	$m3$, $m3m$	23, $\underline{4}3m$, 432

Fig. 2.2 Matrix of the piezoelectric coefficients for crystals of the tetragonal symmetry (point group 4*mm*)

$$\begin{pmatrix} 0 & 0 & 0 & 0 & d_{15} & 0 \\ 0 & 0 & 0 & d_{15} & 0 & 0 \\ d_{31} & d_{31} & d_{33} & 0 & 0 & 0 \end{pmatrix}$$

dipole moment of the unit cell (in the absence of applied fields). If such *spontaneous polarization* can be reversed by an external (sufficiently high) electric field, the crystal is called *ferroelectric*.

Above a certain temperature T_c (often termed the Curie point), the spontaneous polarization vanishes, and the ferroelectric crystal transforms into the paraelectric state. Many ferroelectrics lose their piezoelectric properties above T_c completely, because their paraelectric phase has centrosymmetric crystallographic structure. The advantage of ferroelectrics, well understood already in the beginning of the last century (while studying Rochelle salt), is that they have much higher piezoelectric activity, especially in the vicinity of the Curie point, where the piezoelectric coefficients increase dramatically. In ferroelectrics with a centrosymmetric paraelectric phase, the piezoelectric coefficients are proportional to the product of polarization and dielectric permittivity and, therefore, should be high in materials having large polarizability and spontaneous polarization. For the tetragonal 4*mm* crystals, the longitudinal piezoelectric coefficient d_{33} can be expressed as

$$d_{33} = 2Q_{11}\varepsilon_0\varepsilon_{33}P_3, \tag{2.3}$$

where ε_{33} and P_3 are the relative permittivity and polarization along the polar x_3 axis, $\varepsilon_0 = 8.854 \times 10^{-12}\,\mathrm{F/m}$ is the permittivity of vacuum, and Q_{11} is the electrostrictive constant of the paraelectric phase, which couples longitudinal strain S_3 and polarization via the equation

$$S_3 = Q_{11}P_3^2. \tag{2.4}$$

The electrostriction coefficient involved in (2.3) practically does not depend on temperature and typically varies between 0.05 and $0.1\,\mathrm{m}^4/\mathrm{C}^2$ for different materials.

The piezoelectric effect was discussed above for the case of single-domain ferroelectric crystals in which the spontaneous polarization is constant everywhere. Another technologically important class of materials is represented by piezoelectric ceramics, which consist of randomly oriented crystallites (grains), separated by grain boundaries. Ceramics are much less expensive in processing than single crystals and frequently offer comparable piezoelectric and electrostrictive properties (Jaffe et al. 1971). It should be emphasized that, in nonferroelectric ceramics, the piezoelectric responses of individual crystallites are canceled out after averaging over the entire sample. Hence, on the macroscopic level, the polycrystal has a center of symmetry and negligible piezoelectric properties.

In contrast, ferroelectric ceramics can be made piezoelectrically active by poling. This feature is due to the presence of so-called *ferroelectric domains* (regions with different orientations of the spontaneous polarization) in as-sintered ferroelectric ceramics. Domains appear in ceramics and single crystals when the material is cooled down through the Curie point in order to minimize the electric and elastic energy of the system.

The boundaries between ferroelectric domains (often called domain walls) can move under the action of applied electric field so that the spontaneous polarization may be reoriented in the crystallographic direction closest to the field direction. As a

result of such poling process, an initially macroscopically centrosymmetric ceramic sample loses the inversion center and becomes piezoelectric. Since it acquires the $\infty\infty m$ symmetry, the poled ceramic has only three independent piezoelectric coefficients d_{33}, d_{31}, and d_{15}, which relate longitudinal, transverse, and shear deformations to the electric field applied along and perpendicular to the poling direction.

The measured piezoelectric response usually contains not only the intrinsic contribution (determined by the lattice properties and described by (2.3)), but also an extrinsic contribution caused by movements of non-180° domain walls. This domain-wall contribution, which will be discussed in detail in Sect. 2.5, depends on the symmetry of ferroelectric material too.

It should be noted that much efforts were made to create materials with enhanced piezoelectric properties. Equation (2.3) suggests that this goal can be achieved by using crystals approaching phase-transition conditions, where the increase of dielectric permittivity should result in high piezoelectric coefficients. The observation of maximum piezoelectric response in PZT solid solutions with compositions close to the morphotropic phase boundary (MPB) gave strong support to this idea long time ago.

Recently, it has been shown that the piezoelectric properties can also be improved by cutting the crystal at some angle to the polarization direction (Park and Shrout 1997). In particular, the solid solutions of $Pb(Zn_{1/3}Nb_{2/3})O_3$ (relaxor ferroelectric) with $PbTiO_3$ (normal ferroelectric) exhibit the highest piezoelectric coefficients along the pseudocubic $\langle 001 \rangle$ direction, while the spontaneous polarization is parallel to the $\langle 111 \rangle$ axis in the rhombohedral PZN–PT crystals studied.

The difference between the piezoelectric responses measured in the [001] and [111] directions is very large in these crystals (see Table 2.2), which may be explained phenomenologically by the orientation dependence of the piezoelectric effect (see Sect. 2.3). On the microscopic scale, the origin of ultrahigh piezoelectricity in PZN–PT solid solutions was attributed to the existence of a monoclinic phase near the MPB separating stability ranges of the rhombohedral and tetragonal states (Noheda et al. 2001). This intermediate monoclinic phase has the b_m axis oriented along the pseudocubic [010] direction and facilitates the polarization rotation between the $\langle 111 \rangle$ and $\langle 001 \rangle$ directions under the influence of electric field applied along the [001] crystallographic axis.

Table 2.2 Physical properties of major piezoelectric materials together with their symmetries

Parameter	Quartz	$BaTiO_3$	$PbTiO_3$: Sm	PZT 5H	LF4T	PZN–8%PT [001]	PZN–8%PT [111]
Symmetry	32	$4mm$	$4mm$	$3m/4mm$	$mm2/4mm$	$3m/4mm$	$3m/4mm$
d_{33}(pC/N)	2.3	190	65	593	410	2500	84
d_{31}(pC/N)	0.09	0.38	0	−274	−154	−1400	−20
$\varepsilon_{33}^T/\varepsilon_0$	5	1700	175	3400	2300	7000	1000
T_c(°C)		120	355	193	253	160	160

2.3 Orientation Dependence of Piezoelectric Response in Single Crystals

The piezoelectric coefficients d^*_{ijk} in an arbitrary coordinate system $(\tilde{x}_1,\tilde{x}_2,\tilde{x}_3)$ can be calculated from the coefficients d_{lmn} defined in the crystallographic reference frame (x_1,x_2,x_3) using the general relation (Cady 1964, Nye 1957)

$$d^*_{ijk} = A_{il}A_{jm}A_{kn}d_{lmn}, \tag{2.5}$$

where A_{il} are the elements of the transformation matrix **A** relating two sets of the coordinate axes. This formula makes it possible to predict the orientation dependence of the piezoelectric properties for any crystal with known piezoelectric coefficients d_{lmn}. In particular, the longitudinal piezoelectric coefficient d^*_{33} measured in the direction making an angle θ with the polar axis of the tetragonal crystal with 4*mm* symmetry can be evaluated as (Nye 1957)

$$d^*_{33} = \cos\theta[\sin^2\theta(d_{15}+d_{31})+\cos^2\theta d_{33}]. \tag{2.6}$$

It can be seen that, when the angle θ increases, the relative contribution of the longitudinal coefficient d_{33} decreases, whereas the contribution of the shear coefficient d_{15} increases. If the sum $d_{15}+d_{31}$ is much larger than d_{33}, the maximum value of $d^*_{33}(\theta)$ corresponds to a direction different from the polar one (Davis et al. 2007). This feature is characteristic of $BaTiO_3$ at room temperature $[(d_{15}+d_{31})/d_{33} \approx 6]$, where it exhibits maximum longitudinal piezoelectric response close to the [111] direction (Damjanovic et al. 2002). In contrast, when the ratio $(d_{15}+d_{31})/d_{33}$ is smaller than some critical value, the maximum response d^*_{33} will be observed along the polar crystallographic axis $(\theta = 0)$ (Davis et al. 2007). The aforementioned two different types of the orientation dependence are illustrated in Fig. 2.3, where $d^*_{33}(\theta)$ is plotted for $BaTiO_3$ and $PbTiO_3$ $[(d_{15}+d_{31})/d_{33} \approx 0.4]$ at room temperature.

The orientation dependence of d^*_{33} becomes more complex for piezoelectric crystals of other symmetries. In the case of an orthorhombic *mm*2 crystal, the coefficient d^*_{33} is a function of two Euler angles, θ and ϕ. Variation of d^*_{33} with these angles is described by the relation (Nye 1957)

$$d^*_{33} = \cos\theta[\sin^2\theta\sin^2\phi(d_{15}+d_{31})+\sin^2\theta\cos^2\phi(d_{24}+d_{32})+\cos^2\theta d_{33}]. \tag{2.7}$$

Again, the maximum piezoelectric response will be observed away from the polar direction if one of the shear coefficients is large compared with d_{33}. This happens, for instance, in $KNbO_3$ and PZN–9%PT crystals (Davis et al. 2007).

For the rhombohedral 3*m* crystal, the longitudinal piezoelectric coefficient measured in an arbitrary direction can be evaluated as

$$d^*_{33} = \cos\theta\sin^2\theta\sin^2\phi(d_{31}+d_{15})+\sin^3\theta\cos\phi(3\sin^2\phi-\cos^2\phi)d_{22}+\cos^3\theta d_{33}. \tag{2.8}$$

It can be seen that at $\phi = 90^\circ$ the contribution of the coefficient d_{22} becomes zero, and the orientation dependence of d^*_{33} reduces to that discussed above for

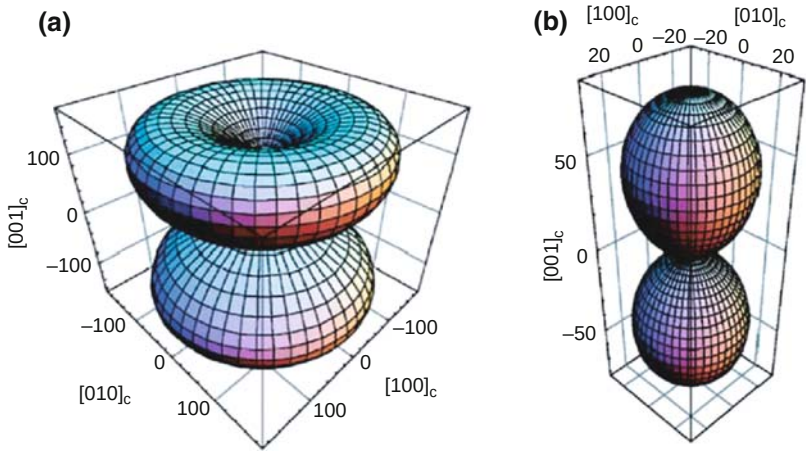

Fig. 2.3 Longitudinal piezoelectric coefficient d_{33}^* (pm/V) as a function of the measuring direction in $BaTiO_3$ (**a**) and $PbTiO_3$ (**b**) at room temperature. The spontaneous polarization is oriented along the (vertical) [001] crystallographic axis. (Reprinted with permission from Davis et al. 2007. Copyright 2007, American Institute of Physics.)

the tetragonal 4*mm* crystals. The calculations performed for PMN–33%PT crystals $((d_{15}+d_{31})/d_{33} \approx 21)$ indeed showed that the maximum value of d_{33}^* corresponds to a direction rotated by 63° away from the polarization direction (Zhang et al. 2003). The orientation dependence of this type is also expected for several other rhombohedral 3*m* crystals, including PZN–7%PT and rhombohedral PZT compositions (Davis et al. 2007).

Remarkably, the giant piezoelectric response of PZN–PT and PMN–PT relaxor-ferroelectric single crystals is observed along nonpolar directions (Park and Shrout 1997). In rhombohedral PZN–8%PT, for example, extremely large $d_{33}^* \sim 2500\,\mathrm{pC/N}$ corresponds to the $\langle 001 \rangle$ crystallographic direction, whereas the piezoelectric coefficient measured along the polar $\langle 111 \rangle$ axis is only about 80 pC/N (Park and Shrout 1997). Accordingly, the giant piezoelectric properties of PZN–PT and PMN–PT may be attributed to the field-induced polarization rotations (Fu and Cohen 2000). Such rotations are expected to be especially easy in the presence of monoclinic phases existing at the MPB regions of PZN–PT, PMN–PT, and PZT (Cox et al. 2001; Ye et al. 2001; Noheda et al. 1999). Indeed, the polarization vector in the M_A (M_B) and M_C monoclinic states can rotate freely in the $\{101\}$ and $\{010\}$ mirror planes (Vanderbilt and Cohen 2001). It is worth noting that the dominant role of polarization rotations in the high piezoelectric response of PZT ceramics with compositions close to MPB was demonstrated by in situ X-ray diffraction measurements (Guo et al. 2000).

It should be emphasized that relative magnitude of the shear piezoelectric coefficient d_{15} is directly related to the dielectric anisotropy of a ferroelectric crystal (Davis et al. 2007). The ratio d_{15}/d_{33} can be written as

$$\frac{d_{15}}{d_{33}} = 2\frac{Q_{1313}}{Q_{3333}}\frac{\eta_{11}}{\eta_{33}}, \tag{2.9}$$

where Q_{1313} and Q_{3333} represent the electrostrictive coefficients defined in the reference frame of the ferroelectric phase, and η_{11} and η_{33} are the transverse and longitudinal dielectric susceptibilities of the single-domain ferroelectric crystal. It can be seen that high dielectric anisotropy of the form $\eta_{11} \gg \eta_{33}$ will normally result in a shear piezoelectric coefficient large compared with d_{33}. The effect of dielectric anisotropy, however, is less pronounced in the tetragonal crystals than in the orthorhombic and rhombohedral ones since the ratio $2Q_{1313}/Q_{3333}$ is only about 0.3–0.4 in common 4*mm* ferroelectrics, whereas it is about 3 or even larger in the *mm*2 and 3*m* ones (Davis et al. 2007).

The dielectric anisotropy may become very large near structural phase transitions between two different ferroelectric phases (Budimir et al. 2003). This enhancement leads to strong increase of the shear piezoelectric response in the vicinity of ferroelectric–ferroelectric transformations induced by temperature or composition variations. Hence, near the morphotropic phase boundaries the longitudinal piezoelectric response d_{33}^* in nonpolar directions should increase strongly as well. The fundamental reason for such piezoelectric anomalies lies in the flattening of the free energy profile in close vicinity to a structural phase transition (Fu and Cohen 2000; Budimir et al. 2006).

2.4 Effective Piezoelectric Constants of Polydomain Crystals, Ceramics, and Thin Films

Ferroelectric crystals usually consist of many domains differing by the spatial orientation of the spontaneous polarization $\mathbf{P}_s$. Inside dissimilar domains, therefore, the local piezoelectric responses to a given external field are generally different. As a result, the piezoelectric properties of polydomain crystals are determined on the macroscopic scale by the average response of the domain ensemble. These "aggregate" material properties, in general, depend on the relative volume fractions of various ferroelectric domains formed in a crystal and on the orientation of domain walls between them.

The set of domain variants permissible in a certain crystal is defined by the crystal symmetry (Aizu 1969). The energetically most favorable orientations of ferroelastic domain walls are determined by the compatibility of spontaneous lattice strains at the wall (Fousek and Janovec 1969; Sapriel 1975). In the presence of ferroelectric polarization $\mathbf{P}$, additional electrical condition must be satisfied, ensuring the absence of polarization charges $\rho = -\mathrm{div}\,\mathbf{P}$ on the wall (Fousek and Janovec 1969). In the case of a tetragonal crystal such as $PbTiO_3$ or $BaTiO_3$ at room temperature, purely ferroelectric 180° walls and ferroelectric–ferroelastic 90° walls are only possible, the latter being oriented, e.g., parallel to the $\{101\}$ crystallographic planes of the prototypic cubic lattice. The orthorhombic phase polarized along the $\langle 110 \rangle$

crystallographic direction may contain 180° walls, 90° walls parallel to the (100) crystallographic plane, 120° walls having the $\{110\}$ orientation, and 60° domain walls with an irrational normal. In the rhombohedral crystal such as $Pb(Zr_{1-x}Ti_x)O_3$ with $x < 0.48$ polarized along the $\langle 111 \rangle$ direction, only the 180° walls and the 71° or 109° walls are possible.

The effective elastic, dielectric, and piezoelectric constants of a polydomain crystal may be calculated from the material constants of a single-domain single crystal for the given geometry of the domain structure. For tetragonal $BaTiO_3$ and $PbTiO_3$ crystals with the laminar 90° domain structure, the effective material constants were determined by Turik (1970) with the aid of an averaging procedure taking into account the mechanical and electrical conditions fulfilled on the domain walls. Remarkably, it was found that the matrix of these constants corresponds to the orthorhombic crystal symmetry rather than the tetragonal one. Similar calculations of the effective piezoelectric coefficients d^*_{3j} performed later for polydomain PMN–33%PT crystals showed that these coefficients strongly depend on the domain concentrations (Topolov 2004). The piezoelectric properties of "domain-engineered" perovskite single crystals were studied in detail by Davis et al. (2005). The tetragonal (point group $4mm$), orthorhombic $(mm2)$, and rhombohedral $(3m)$ crystal phases poled along various crystallographic directions were considered, and the effective piezoelectric coefficient d^*_{31} has been evaluated for polydomain $BaTiO_3$, $PbTiO_3$, $KNbO_3$, and PMN–33%PT crystals.

In the case of ferroelectric ceramics, the aggregate material properties are affected by the elastic, electric, and piezoelectric interactions between individual crystallites (Aleshin and Pikalev 1990; Nan and Clarke 1996; Pertsev et al. 1998a). Indeed, the piezoelectric crystallite is not free to deform under the action of an external electric field because of the elastic clamping imposed by surrounding grains. Besides, the field-induced polarization charges appear at the grain boundaries since the dielectric permittivity usually differs in the adjacent crystallites owing to different lattice orientations. As a result, internal electric fields and mechanical stresses arise (or change) during the piezoelectric measurements, thus making local responses of crystallites different from those of a stress-free electroded single crystal.

The effective piezoelectric constants of ferroelectric ceramics can be calculated theoretically using the so-called effective medium approach or self-consistent scheme (Nan and Clarke 1996; Pertsev et al. 1998a). This approach is based on the introduction of a model material system consisting of a representative crystallite (inclusion) surrounded by a dissimilar homogeneous piezoelectric medium (matrix). In the linear theory, the crystallite (usually assumed to be spherical) is characterized by the small-signal elastic, dielectric, and piezoelectric properties, independent of the internal stresses and electric fields. These properties are determined by the material constants (measured or calculated) of a single-domain or polydomain single crystal. In turn, the matrix parameters represent the unknown macroscopic elastic, piezoelectric, and dielectric constants of a polycrystalline sample, which should be calculated self-consistently by the method of successive approximations.

The numerical calculations performed for $BaTiO_3$ and $PbTiO_3$ ceramics indicated that the aggregate piezoelectric properties of ferroelectric ceramics may experience nonmonotonic variations with the increase of the remanent polarization P_r (Pertsev et al. 1998a). It was found that the piezoelectric constants d_{33}^* and d_{31}^* of $BaTiO_3$ ceramics reach their extreme values at $P_r/P_s \approx 0.87$ and 0.7, respectively. In the case of $PbTiO_3$ ceramics, these piezoelectric coefficients vary monotonically with the remanent polarization, but the constant d_{15}^* displays an absolute maximum at $P_r/P_s \approx 0.95$, where it slightly exceeds the single-crystal value of this constant. Thus, the influence of poling on the piezoelectric properties of ferroelectric ceramics may be different for dissimilar materials.

The elastic clamping of crystallites in a ferroelectric polycrystal not only changes the small-signal aggregate properties, but also modifies lattice strains and the spontaneous polarization. This mechanical effect is expected to be most pronounced in nanocrystalline ceramics, where the twinning of crystallites (formation of ferroelastic domains), which strongly reduces internal stresses, is energetically unfavorable because of a very small grain size (Pertsev and Salje 2000). The equilibrium polarization states of $BaTiO_3$ and $Pb(Zr_{1-x}Ti_x)O_3$ ceramics with single-domain grains were predicted recently using the nonlinear thermodynamic theory combined with the method of effective medium (Zembilgotov et al. 2005). The calculations showed that, owing to the elastic clamping of crystallites, the phase states of nanocrystalline ceramics may differ drastically from those of single crystals and coarse-grained materials. Remarkably, the theory predicted the coexistence of rhombohedral and tetragonal crystallites in nanocrystalline $Pb(Zr_{1-x}Ti_x)O_3$ ceramics in a wide range of compositions and temperatures. For $BaTiO_3$ ceramics, a mixture of rhombohedral and orthorhombic crystallites was found to be the energetically most favorable state at room temperature. Thus, the elastic clamping can change the symmetry of ferroelectric state in a small grain. This result indicates that nanocrystalline ferroelectric ceramics may have specific piezoelectric properties.

The current trend toward the miniaturization of electromechanical systems requires the use of piezoelectric materials in the thin-film form (Muralt 2000). The piezoelectric response of a thin film grown on a dissimilar thick substrate may be very different from that of a bulk material. The most evident reason for such a difference is the two-dimensional (2D) clamping of the film by the rigid substrate (Lefki and Dormans 1994). Since the in-plane dimensions of the film are fixed while the film thickness is free to change under the action of applied electric field E_3, the effective longitudinal piezoelectric coefficient d_{33}^f of a thin film can be evaluated as (Lefki and Dormans 1994)

$$d_{33}^f = d_{33} - \frac{2s_{13}^E}{s_{11}^E - s_{12}^E} d_{31}, \tag{2.10}$$

where d_{in} are the piezoelectric constants of a bulk material, and s_{mn}^E are the bulk elastic stiffnesses at constant electric field. The effective transverse piezoelectric coefficient e_{31}^f, which defines the stresses σ_1 and σ_2 induced in the film plane by the electric field E_3, is defined by a similar relation

$$e_{31}^{\mathrm{f}} = e_{31} - \frac{c_{13}^{\mathrm{E}}}{c_{33}^{\mathrm{E}}} e_{33}, \tag{2.11}$$

where c_{mn}^{E} are the bulk elastic compliances (Muralt 2000). It can be seen that e_{31}^{f} is always larger than the bulk coefficient e_{31}, whereas d_{33}^{f} is smaller than d_{33}. Indeed, it is implied here that the film piezoelectric and elastic constants do not differ significantly from those of the bulk material, which is a reasonable assumption for ordinary piezoelectrics, but not necessarily for ferroelectric materials (see below).

In addition to the 2D clamping, the film is usually strained by the substrate to a certain extent (e.g., because of the difference in the thermal expansion coefficients). Since in ferroelectrics the polarization is coupled to lattice strains via the electrostriction, the substrate-induced strains may change the piezoelectric properties of ferroelectric films markedly. In the case of polycrystalline thin films of multiaxial ferroelectrics, the mechanical substrate effect usually induces preferential orientations for the polar axes of crystallites, which results in the formation of a crystal texture below the phase transition temperature T_{c} (Pertsev et al. 1998a). When the substrate induces compressive in-plane stresses σ_1 and σ_2 above T_{c}, polycrystalline films of perovskite ferroelectrics such as $BaTiO_3$, $PbTiO_3$, and $Pb(Zr_{1-x}Ti_x)O_3$ acquire the *c*-texture with the polar axes oriented as close as possible to the substrate normal. In the films grown on "tensile" substrates $(\sigma_1, \sigma_2 > 0)$, the *a*-texture is formed, where directions of the polar axes have minimum possible deviations from the film plane. Evidently, the *c*- and *a*-textured films will behave quite differently during the poling process and so exhibit different piezoelectric properties.

Owing to the substrate-induced strains, the orientation of the spontaneous polarization in a ferroelectric thin film may also deviate from the polar crystallographic axis in the bulk material (e.g., from the $\langle 001 \rangle$ direction in the tetragonal crystal, the $\langle 101 \rangle$ direction in the orthorhombic crystal, and the $\langle 111 \rangle$ direction in the rhombohedral one). Such polarization rotations are expected to be especially large in the single-crystalline films free of ferroelastic domains (twins). Here the mechanical film–substrate interaction results in the formation of new phases not existing in bulk crystals (Pertsev et al. 1998b, 2000, 2003; Tagantsev et al. 2002). This phenomenon originates in the strain-induced lowering of the symmetry of the paraelectric phase.

In the case of (001)-oriented films of perovskite ferroelectrics grown on (001)-oriented cubic substrates, the strain effect lowers the symmetry of the paraelectric state from cubic to tetragonal (Pertsev et al. 1998b). As a result, five low-temperature phases become theoretically possible in the film instead of three in the bulk crystal. Among these five phases, the most important ones are the tetragonal *c* phase with the polarization $\mathbf{P}_{\mathrm{s}}$ orthogonal to the film surfaces, the orthorhombic *aa* phase with the in-plane polarization, and the monoclinic *r* phase with the vector $\mathbf{P}_{\mathrm{s}}$ inclined to the film surfaces (see Fig. 2.4). The aforementioned three ferroelectric phases were shown to be stable in single-domain $BaTiO_3$, $PbTiO_3$, and $Pb(Zr_{1-x}Ti_x)O_3$ $(x \geq 0.4)$ films under certain strain–temperature conditions (Pertsev et al. 1998b, 2003; Diéguez et al. 2004). The stability ranges of various possible polarization states in ferroelectric films can be conveniently described with the aid of phase diagrams, where the temperature T and the misfit strain S_{m} between the substrate

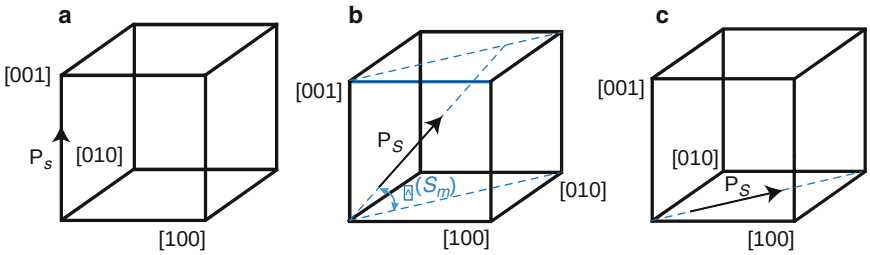

Fig. 2.4 Orientation of the spontaneous polarization $\mathbf{P}_s$ in stable ferroelectric phases forming in (001)-oriented single-domain thin films of perovskite ferroelectrics grown on (001)-oriented cubic substrates: tetragonal *c* phase (**a**), monoclinic *r* phase (**b**), and orthorhombic *aa* phase (**c**). Polarization orientations are shown relative to the prototypic cubic cell

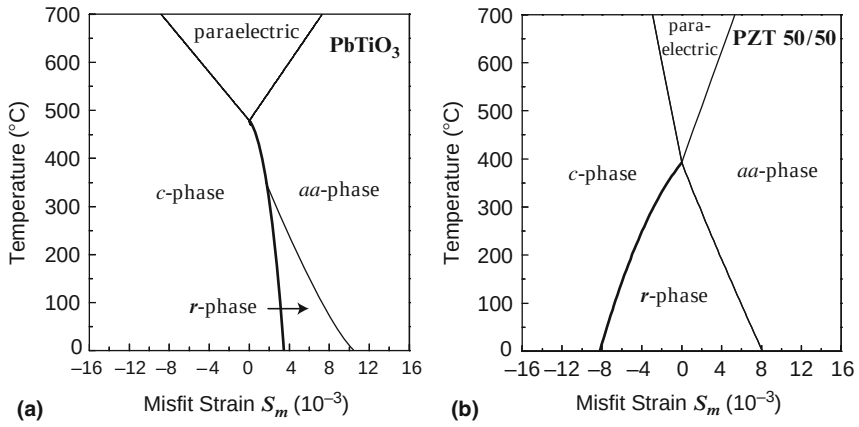

Fig. 2.5 Misfit strain–temperature phase diagrams of (001)-oriented single-domain $PbTiO_3$ (**a**) and $Pb(Zr_{0.5}Ti_{0.5})O_3$ (**b**) films epitaxially grown on (001)-oriented cubic substrates The first- and second-order phase transitions are shown by thick and thin lines, respectively. (Reprinted with permission from Pertsev et al. 1998b and 2003. Copyright 1998, 2003, American Physical Society.)

and the film prototypic cubic state are used as two independent variables (Pertsev et al. 1998b). Representative misfit strain–temperature phase diagrams of perovskite ferroelectric films are shown in Fig. 2.5. It can be seen that the diagrams of single-domain $PbTiO_3$ and $Pb(Zr_{0.5}Ti_{0.5})O_3$ films contain large stability ranges of the orthorhombic and monoclinic phases, which do not exist in the corresponding bulk materials.

The small-signal piezoelectric properties of epitaxial ferroelectric films evidently depend on the film polarization state. Hence the piezoelectric coefficients are functions of the misfit strain S_m in the film–substrate system, which can be determined using the film (S_m, T) phase diagram. Figure 2.6a shows a representative strain dependence of the longitudinal piezoelectric coefficient d_{33}, which was calculated for single-domain $Pb(Zr_{0.4}Ti_{0.6})O_3$ films using the nonlinear thermodynamic theory (Pertsev et al. 2003). Remarkably, d_{33} strongly increases near critical misfit strains

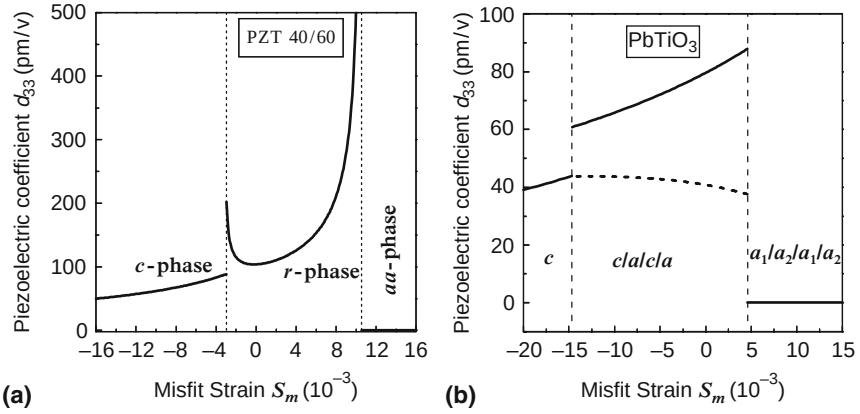

Fig. 2.6 Longitudinal piezoelectric coefficient d_{33} of single-domain $Pb(Zr_{0.4}Ti_{0.6})O_3$ (**a**) and polydomain $PbTiO_3$ (**b**) thin films as a function of the misfit strain in the epitaxial system. The dashed line in (**b**) shows the variation of d_{33} in $PbTiO_3$ film with pinned domain walls. (Reprinted with permission from Pertsev et al. 2003 and Koukhar et al. 2001. Copyright 2001, 2003, American Physical Society.)

at which the monoclinic *r* phase transforms either into the orthorhombic *aa* phase or into the tetragonal *c* phase. On the other hand, ferroelectric films grown on "strongly compressive" or "strongly tensile" substrates exhibit only small or zero piezoelectric response d_{33}.

The substrate-induced lattice strains may partially relax via the formation of elastic domains (twins) in the film (Roitburd 1976). Such relaxation modifies the (S_m, T) phase diagram and hence may change the film piezoelectric response (Koukhar et al. 2001). In $PbTiO_3$ films, the twinning removes the *r* and *aa* phases from the equilibrium diagram (see Fig. 2.7a), because the pseudo-tetragonal *c/a/c/a* and $a_1/a_2/a_1/a_2$ polydomain states appear to be energetically more favorable. As a result, the misfit-strain dependence of d_{33} weakens in a polydomain film, as shown in Fig. 2.7b. In contrast, the monoclinic phase survives in the case of $Pb(Zr_{0.5}Ti_{0.5})O_3$ films (Kukhar et al. 2006), where the monoclinic $r_1/r_2/r_1/r_2$ and $ca_1/ca_2/ca_1/ca_2$ polydomain states are stable at small misfit strains in a wide range of temperatures (see Fig. 2.7b).

2.5 Domain-Wall Contribution to Piezoelectric Coefficients of Ferroelectric Ceramics and Thin Films

The measuring electric field **E** generally exerts a driving force on the domain walls in a ferroelectric material. The field-induced displacements of these walls from their initial positions may change the average lattice strains, thus giving an extrinsic contribution to the piezoelectric response. The domain-wall contribution can be

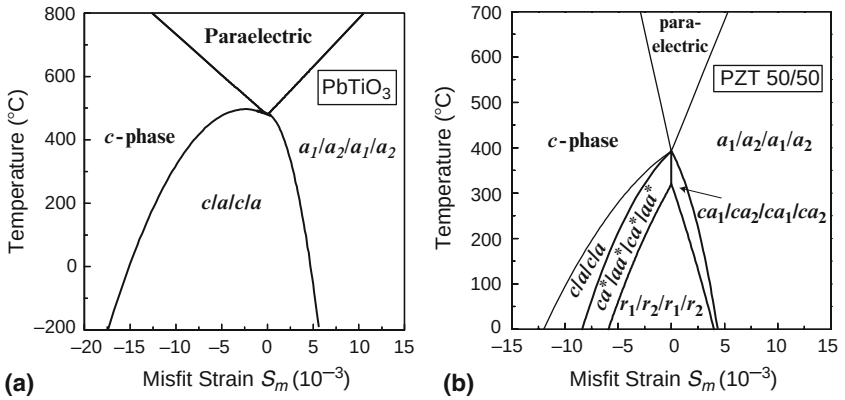

Fig. 2.7 Misfit strain–temperature phase diagrams of (001)-oriented polydomain $PbTiO_3$ (**a**) and $Pb(Zr_{0.5}Ti_{0.5})O_3$ (**b**) films epitaxially grown on (001)-oriented cubic substrates. The first- and second-order phase transitions are shown by thick and thin lines, respectively. (Reprinted with permission from Koukhar et al. 2001 and Kukhar et al. 2006. Copyright 2001, 2006, American Physical Society.)

evaluated theoretically by calculating the average wall displacement δl as a function of the field intensity E_i and determining the strain change δS_n in the volume swept by the moving walls. We shall consider below the domain-wall contribution Δd_{in} to the small-signal piezoelectric constants d_{in} only, assuming that the measuring field is weak ($\mathbf{E} \to 0$).

Since the magnitude δl of domain-wall displacements is directly proportional to the field intensity (see below), a nonnegligible contribution Δd_{in} appears only when the strain change δS_n is independent of the applied field. This requirement demonstrates that displacements of purely ferroelectric domain walls (e.g., 180° walls in tetragonal crystals) do not affect the small-signal piezoelectric response (since $\delta S_3 \sim E_3$). In contrast, the ferroelectric–ferroelastic 90° walls create significant contribution to the piezoelectric coefficients of tetragonal ferroelectric ceramics and thin films (Bondarenko et al. 1990; Arlt and Pertsev 1991; Pertsev and Emelyanov 1997; Koukhar et al. 2001). This contribution results from the collective antiparallel motion of 90° walls forming periodic laminar patterns in these material systems (Arlt 1990; DeVeirman et al. 1993; Ramesh et al. 1993; Kwak et al. 1994). Remarkably, the shift of a 90° wall produces a local strain change proportional to the square of spontaneous polarization P_s.

The magnitude of cooperative displacements of the 90° walls is mainly restricted by the restoring forces associated with the changes of long-range elastic and electric internal fields caused by these displacements. When δl is much smaller than the domain width w, the restoring force acting per unit wall area can be written as $f_{res} = -k\ \delta l$, where k is the force constant. For tetragonal ferroelectric ceramics, the domain-wall contributions to the low-frequency piezoelectric constants can be evaluated as (Arlt and Pertsev 1991)

$$\Delta d_{33} = \frac{(Q_{11} - Q_{12})P_s^3}{k_{cer} w} J_{d_{33}}, \quad \Delta d_{31} = -\frac{1}{2}\Delta d_{33}, \quad \Delta d_{15} = \frac{(Q_{11} - Q_{12})P_s^3}{k_{cer} w} J_{d_{15}}, \tag{2.12}$$

where Q_{mn} are the electrostrictive constants of the paraelectric phase, and J_{din} are the parameters depending on distribution of the grain polarizations among various spatial orientations in a ferroelectric ceramic. The force constant k_{cer} involved in the above relations can be calculated in an analytical form (Arlt and Pertsev 1991). Since k_{cer} is inversely proportional to the domain width w, the contributions Δd_{in} are predicted to be independent of the domain-wall density in the first approximation. The numerical calculations show that Δd_{33} and Δd_{15} are considerable in poled $BaTiO_3$ and PZT ceramics, amounting to about 100 pC/N in $BaTiO_3$ and about 50 pC/N in PZT at the remanent polarization $P_r = 0.35 P_s$ (Arlt and Pertsev 1991).

In the case of epitaxial ferroelectric thin films, significant domain-wall contribution to the coefficient d_{33} appears when the pseudo-tetragonal *c/a/c/a* domain structure forms in the film (Pertsev and Emelyanov 1997; Koukhar et al. 2001). Since the electric field E_3 induced between the top and bottom electrodes covering the film surfaces interacts with the out-of-plane polarization P_3, the *c* domains change their size periodically during the piezoelectric measurements at the expense of the *a* domains having the in-plane spontaneous polarization. The force constant k_{film} determining the mechanical restoring force acting on displaced 90° c/a walls can be calculated analytically in the linear elastic approximation, which make it possible to evaluate the domain-wall contribution Δd_{33} (Pertsev and Emelyanov 1997). For relatively thick films (thickness > 100 nm), where the widths of *c* and *a* domains become much smaller than the film thickness ("dense" domain structure), Δd_{33} is given by a simple relation

$$\Delta d_{33} = \frac{(s_{11} + 2s_{12})(s_{11} - s_{12})}{s_{11}(Q_{11} - Q_{12})P_s}, \tag{2.13}$$

where s_{nm} are the elastic compliances at constant polarization. This relation shows that Δd_{33} is expected to be significant in poled thin films of conventional perovskite ferroelectrics ($\Delta d_{33} \approx 100\,\mathrm{pm/V}$ in $BaTiO_3$ films and about 50 pm/V in $PbTiO_3$ films). The accurate numerical calculations performed with the aid of the nonlinear thermodynamic theory (Koukhar et al. 2001) demonstrated that actually the domain-wall contribution depends on the misfit strain in the film–substrate system (see Fig. 2.7b). Moreover, they confirmed that Δd_{33} is comparable with the intrinsic contribution to the film piezoelectric response.

Since the calculations discussed above ignore the interactions of domain walls with crystal defects and the lattice periodic potential (Peierls potential relief), they give only the upper bound for the domain-wall contribution to the piezoelectric response. Although the Peierls barriers for ferroelastic domain walls should be relatively small (because the thickness of such walls is usually much larger than the lattice period; see Chrosch and Salje 1999), at low temperatures they could reduce Δd_{33} considerably (Kukhar et al. 2006). Nevertheless, the domain-wall contribution

to the piezoelectric coefficients of multiaxial polydomain ferroelectrics in general cannot be ignored. It should be noted that the field-induced displacements of the c/a domain walls were confirmed experimentally for $Pb(Zr_{0.32}Ti_{0.68})O_3$ thin films grown on MgO (Lee et al. 2001).

2.6 Piezoelectric Effect and Magnetism

Recent years witnessed the advent of novel materials that combine piezoelectric (linear in external stimulus) response with other attractive functionalities such as magnetic activity. Remarkably, the coupling between electric and magnetic variables is permitted only in crystals of certain symmetries. Such coupling is not only of high fundamental interest, but also of practical importance since it could be used to create new types of nonvolatile memories, where the data are written electrically and read magnetically (Eerenstein et al. 2006). It should be emphasized that piezoelectricity may also lead to the magnetoelectric coupling if the material simultaneously exhibits *piezomagnetism*. Indeed, the application of an electric field to such material induces strain via the converse piezoelectric effect, which, in turn, changes the magnetization because of the direct piezomagnetic effect. Similarly, the magnetic field creates lattice strains via the converse piezomagnetic effect so that the polarization also changes because of the direct piezoelectric effect.

Piezomagnetism is a linear effect relating strain and magnetic field or stress and magnetization. A strain S_{ik} produces a magnetic field $H_i = -\lambda_{ijk}S_{jk}$, where λ_{ijk} is the third-rank tensor. In turn, a magnetic field may produce strain (converse piezomagnetic effect). Similar to all magnetic tensors (see, e.g., Nye 1957), λ_{ijk} vanishes in all crystals symmetric with respect to the time inversion. Also, it is symmetric with respect to the last two indices, analogously to the piezoelectric tensor. The piezomagnetic effect is absent in the magnetic classes $m3m$, $\underline{4}3m$, and 432. Despite the piezomagnetic effect is typically small, it is used, for example, to register earthquakes. Strong coupling between piezoelectric and magnetic phenomena is expected in the materials called multiferroics that recently attracted a lot of interest in both magnetic and ferroelectric communities (Eerenstein et al. 2006; Cheong and Mostovoy 2007; Ramesh and Spaldin 2007).

Multiferroic crystals are distinguished by the simultaneous presence of two different order parameters such as polarization and magnetization (see, for example, a recent review (Fiebig 2005)). The crystal symmetry imposes a strict limitation on this class of materials (Aizu 1970, Schmid 1994). There are four major crystallographic types of multiferroics:

1. *Compounds with perovskite structure*. They have the chemical formula ABO_3 or $A_2B'B''O_6$. For example, the well-known compound $BiFeO_3$ is ferroelectric, ferroelastic, and weakly ferromagnetic at room temperature. It is rhombohedrally distorted with the crystallographic point symmetry $3m$.
2. *Compounds with hexagonal structure*. These compounds also have the chemical formula ABO_3 or $A_2B'B''O_6$. The hexagonal structure is due to relatively small

cationic radii. Ferroelectric–antiferromagnetic manganites $R\mathrm{MnO_3}$, with $R = $ Sc, Y, In, Ho, Er, Yb, or Lu, form a large group of hexagonal multiferroics. They have the crystallographic point symmetry 6*mm*.

3. *Boracites*. They have the general formula $M_3\mathrm{B_7O_{13}}X$. These crystals are ferroelectric–ferroelastic antiferromagnets (in some cases with a small ferromagnetic moment). Here $M = $ Cr, Mn, Fe, Co, Cu, or Ni and $X = $ Cl or I. Boracites are cubic with the point symmetry $\underline{4}3m$ at high temperatures and the $3m$ point group in the ferroelectric phase.
4. *Compounds with* $\mathrm{Ba}M\mathrm{F_4}$ *structure*. $M = $ Mg, Mn, Fe, Co, Ni, or Zn. These compounds are orthorhombic with the 2*mm* point symmetry at high temperatures. At low temperatures, they are ferroelastic ferroelectrics with a small ferromagnetic moment.

In addition, there is a large number of multiferroics with other structures (Eerenstein et al. 2006; Cheong and Mostovoy 2007). Basic symmetries of ferroelectrics, ferromagnets, ferroelastics, and multiferroics are compared in Table 2.3.

Appearance of spontaneous polarization and spontaneous magnetization breaks the spatial-inversion and time-reversal symmetries in multiferroics at low temperatures. This results in a linear magnetoelectric effect that involves both magnetic and electric fields: A magnetic field **H** induces an electric polarization **P** with components $P_i = \alpha_{ij}H_j$, and, in turn, an electric field **E** induces a magnetization **M** with components $M_i = \alpha_{ji}E_j$. Table 2.3 shows that the tensor α_{ij} can be nonzero only in materials that are noncentrosymmetric and time-asymmetric. There is a strict upper bound for the coefficients α_{ij} : $\alpha_{ij}^2 < \eta_{ii}\mu_{jj}$ (Brown et al. 1968). The linear magnetoelectric effect is small in most of the materials because either the dielectric (η_{ii}) or magnetic (μ_{jj}) susceptibility has a small value.

In the perovskite multiferroics, the crystal symmetry permits the linear magnetoelectric effect $(\alpha_{ij} \neq 0)$ and the existence of a spontaneous polarization **P** and a spontaneous magnetization **M**. For example, let us consider $\mathrm{BiFeO_3}$. The free energy of this compound must be invariant with respect to the spatial inversion and rotations by the angle of 120° around the z axis. Therefore, the free energy F can be expressed through the corresponding invariants. The invariant $E_z(M_yL_x - M_xL_y)$, where **L** is the vector of the antiferromagnetic order, permits a spontaneous polarization along the z axis:

$$\mathbf{P} = -\frac{\partial F}{\partial \mathbf{E}} \propto (0, 0, M_yL_x - M_xL_y). \tag{2.14}$$

Table 2.3 Symmetry requirements for ferroics

Ferroic	Spatial-inversion symmetry?	Time-reversal symmetry?
Ferroelastic	Yes	Yes
Ferroelectric	No	Yes
Ferromagnetic	Yes	No
Multiferroic	No	No

Reprinted with permission from Eerenstein et al. 2006. Copyright 2006, Nature Publishing Group

The invariant $P_z(H_yL_x - H_xL_y)$ permits a spontaneous magnetization

$$\mathbf{M} = -\frac{\partial F}{\partial \mathbf{H}} \propto (P_zL_y, -P_zL_x, 0). \tag{2.15}$$

Using these invariants, one can also show that the magnetoelectric effect is nonzero ($\alpha_{ij} \neq 0$). However, the disadvantage of these compounds is that they may have an incommensurate magnetic structure. In $BiFeO_3$, the spins of Fe ions form a long-wavelength ($\lambda = 62\,\mathrm{nm}$) spiral structure. Averaging over the whole sample leads to zero magnetoelectric effect. This effect may be restored by applying strong magnetic field ($H \sim 20\,\mathrm{T}$) or by chemical substitution.

In contrast to perovskite multiferroics, the crystal symmetry of hexagonal manganites $R\mathrm{MnO_3}$ forbids the linear magnetoelectric effect. In these compounds, the interaction between electric and magnetic moments may arise via the piezomagnetic effect, which couples magnetization with the strain induced by electric polarization (Fiebig et al. 2002). Introduction of the strain coupling represents an attractive method for engineering an enhanced magnetoelectric effect.

In boracite $Ni_3B_7O_{13}I$, weak magnetic and electric orders emerge simultaneously below 60 K. The magnetoelectric effect is permitted. Applying a magnetic field, one can induce reversal of the magnetization, which, in turn, flips the polarization. In $BaMnF_4$, a spontaneous magnetoelectric effect is permitted owing to the presence of a weak permanent magnetization. Unfortunately, high magnitude of the electric coercive field renders the manipulation of the polarization difficult because this requires the application of a very strong magnetic field.

Recent findings showed that magnetoelectric, piezomagnetic, magnetoelastic, and other cross-coupling effects relating electrical, mechanical, and magnetic phenomena are typically weak in single-phase materials. In composites, however, they may be much stronger (Dong et al. 2002; Zheng et al. 2004; Eerenstein et al. 2006), especially near the phase-transition temperatures. The symmetry considerations can be very useful for finding a good combination of piezoelectric–ferroelectric and magnetostrictive–ferromagnetic materials. Another interesting opportunity is offered by the large coupling effects found within antiferromagnetic–ferroelectric domain walls (Fiebig et al. 2002).

2.7 Conclusion

Based on the above discussion, we can conclude that the piezoelectric effect in crystalline materials to a large extent is defined by the crystal symmetry. The symmetry considerations are indispensable for understanding the piezoelectric properties of single crystals, ceramics, and thin films. By varying the orientation of the applied field with respect to the crystallographic axes, it is possible to enhance the piezoelectric response of some crystals drastically. This orientation dependence of the piezoelectric properties is especially strong in crystals of the relaxor ferroelectrics. The effective piezoelectric coefficients of ferroelectric ceramics and thin films strongly

depend on the spatial orientations of polar axes in crystallites and domains as well. Finally, it should be emphasized that crystallographic symmetry imposes strict limitations on the piezoelectric crystals, which could be simultaneously magnetically active.

Acknowledgments This work was partly supported by the EU-funded project "Multiceral" (NMP3-CT-2006-032616). N.A.P. acknowledges the Erasmus Mundus programme of the European Commission for financial support.

References

Aizu K (1969) Possible species of "ferroelastic" crystals and of simultaneously ferroelectric and ferroelastic crystals. J Phys Soc Jpn 27:387

Aizu K (1970) Possible species of ferromagnetic, ferroelectric, and ferroelastic crystals. Phys Rev B 2:754–772

Aleshin VI, Pikalev EM (1990) Effect of internal mechanic tensions on properties of ferroceramics. Zh Tekh Fiz 60:129–134

Arlt G (1990) Twinning in ferroelectric and ferroelastic ceramics – stress relief. J Mater Sci 25:2655–2666

Arlt G, Pertsev NA (1991) Force constant and effective mass of 90° domain walls in ferroelectric ceramics. J Appl Phys 70:2283–2289

Bondarenko EI et al. (1990) The effect of 90° domain wall displacements on piezoelectric and dielectric constants of perovskite ferroelectric ceramics. Ferroelectrics 110:53–56

Brown WF et al. (1968) Upper bound on the magnetoelectric susceptibility. Phys Rev 168:574–577

Budimir M et al. (2003) Piezoelectric anisotropy–phase transition relations in perovskite single crystals. J Appl Phys 94:6753–6761

Budimir M et al. (2006) Piezoelectric response and free-energy instability in the perovskite crystals $BaTiO_3$, $PbTiO_3$, and $Pb(Zr,Ti)O_3$. Phys Rev B 73:174106

Cady WG (1964) Piezoelectricity. Dover, New York

Cheong SW, Mostovoy M (2007) Multiferroics: A magnetic twist for ferroelectricity. Nat Mater 6:13–20

Chrosch J, Salje EKH (1999) Temperature dependence of the domain wall width in $LaAlO_3$. J Appl Phys 85:722–727

Cox DE et al. (2001) Universal phase diagram for high-piezoelectric perovskite systems. Appl Phys Lett 79:400–402

Curie P, Curie J (1880) Développement, par pression, de l'électricité polaire dans les cristaux hémièdres à faces inclinées. Comptes Rendus (France) 91:294–295

Curie P, Curie J (1881) Contractions et dilatations produites par des tensions électriques dans les cristaux hémièdres à faces inclinées. Comptes Rendus (France) 93:1137–1140

Damjanovic D et al. (2002) Crystal orientation dependence of the piezoelectric d_{33} coefficient in tetragonal $BaTiO_3$ as a function of temperature. Appl Phys Lett 80:652–654

Davis M et al. (2005) Domain engineering of the transverse piezoelectric coefficient in perovskite ferroelectrics. J Appl Phys 98:014102

Davis M et al. (2007) Rotator and extender ferroelectrics: Importance of the shear coefficient to the piezoelectric properties of domain-engineered crystals and ceramics. J Appl Phys 101:054112

DeVeirman AEM et al. (1993) TEM and XRD characterization of epitaxially grown $PbTiO_3$ prepared by pulsed-laser deposition. Philips J Res 47:185–201

Diéguez O et al. (2004) Ab initio study of the phase diagram of epitaxial $BaTiO_3$. Phys Rev B 69:212101

Dong SX et al. (2002) Circumferentially magnetized and circumferentially polarized magnetostrictive/piezoelectric laminated rings. J Appl Phys 96:3382–3387
Eerenstein W et al. (2006) Multiferroic and magnetoelectric materials. Nature 442:759–765
Fiebig M (2005) Revival of the magnetoelectric effect. J Phys D: Appl Phys 38:R123–152
Fiebig M et al. (2002) Observation of coupled magnetic and electric domains. Nature 419:818–820
Fousek J, Janovec V (1969) The orientation of domain walls in twinned ferroelectric crystals. J Appl Phys 40:135–142
Fu H, Cohen RE (2000) Polarization rotation mechanism for ultrahigh electromechanical response in single-crystal piezoelectrics. Nature 403:281–283
Guo R et al. (2000) Origin of the high piezoelectric response in $PbZr_{1-x}Ti_xO_3$. Phys Rev Lett 84:5423–5426
Jaffe B, Cook WR, Jaffe H (1971) Piezoelectric Ceramics. Academic Press, New York
Koukhar VG et al. (2001) Thermodynamic theory of epitaxial ferroelectric thin films with dense domain structures. Phys Rev B 64:214103
Kukhar VG et al. (2006) Polarization states of polydomain epitaxial $Pb(Zr_{1-x}Ti_x)O_3$ thin films and their dielectric properties. Phys Rev B 73:214103
Kwak BS et al. (1994) Domain formation and strain relaxation in epitaxial ferroelectric heterostructures. Phys Rev B 49:14865–14879
Lee KS et al. (2001) In situ observation of ferroelectric 90°-domain switching in epitaxial $Pb(Zr, Ti)O_3$ thin films by synchrotron X-ray diffraction. Appl Phys Lett 79:2444–2446
Lefki K, Dormans G J M (1994) Measurement of piezoelectric coefficients of ferroelectric thin films. J Appl Phys 76:1764–1767
Lippmann G (1881) Principe de la conservation de l'elecricité. Ann de Chemie e de Physique (5 serie) 24:145
Muralt P (2000) Ferroelectric thin films for micro-sensors and actuators: A review. J Micromech Microeng 10:136–146
Nan CW, Clarke DR (1996) Piezoelectric moduli of piezoelectric ceramics. J Am Ceram Soc 79:2563–2566
Noheda B et al. (1999) A monoclinic ferroelectric phase in the $Pb(Zr_{1-x}Ti_x)O_3$ solid solution. Appl Phys Lett 74:2059–2061
Noheda B et al. (2001) Polarization rotation via a monoclinic phase in the piezoelectric $92\%PbZn_{1/3}Nb_{2/3}O_3$–$8\%PbTiO_3$. Phys Rev Lett 86:003891
Nye JF (1957) Physical Properties of Crystals. Clarendon Press, Oxford
Park S-E, Shrout TR (1997) Ultrahigh strain and piezoelectric behavior in relaxor based ferroelectric single crystals. J Appl Phys 82:1804–1811
Pertsev NA, Emelyanov AYu (1997) Domain-wall contribution to the piezoelectric response of epitaxial ferroelectric thin films. Appl Phys Lett 71:3646–3648
Pertsev NA, Salje EKH (2000) Thermodynamics of pseudoproper and improper ferroelastic inclusions and polycrystals: Effect of elastic clamping on phase transitions. Phys Rev B 61: 902–908
Pertsev NA et al. (1998a) Aggregate linear properties of ferroelectric ceramics and polycrystalline thin films: Calculation by the method of effective piezoelectric medium. J Appl Phys 84:1524–1529
Pertsev NA et al. (1998b) Effect of mechanical boundary conditions on phase diagrams of epitaxial ferroelectric thin films. Phys Rev Lett 80:1988–1991
Pertsev NA et al. (2000) Phase transitions and strain-induced ferroelectricity in $SrTiO_3$ epitaxial thin films. Phys Rev B 61:R825–R829
Pertsev NA et al. (2003) Phase diagrams and physical properties of single-domain epitaxial $Pb(Zr_{1-x}Ti_x)O_3$ thin films. Phys Rev B 67:054107
Ramesh R, Spaldin N (2007) Mutliferroics: Progress and prospects in thin films. Nat Mater 6:21–28
Ramesh R et al. (1993) Effect of crystallographic orientation on ferroelectric properties of $PbZr_{0.2}Ti_{0.8}O_3$ thin films. Appl Phys Lett 63:731–733
Roitburd AL (1976) Equilibrium structure of epitaxial layers. Phys Status Solidi A 37:329–339
Sapriel J (1975) Domain-wall orientations in ferroelastics. Phys Rev B 12:5128–5140
Schmid H (1994) Multiferroic magnetoelectrics. Ferroelectrics 162:317–338

Tagantsev AK et al. (2002) Strain-induced diffuse dielectric anomaly and critical point in perovskite ferroelectric thin films. Phys Rev B 65:012104

Topolov VYu (2004) The remarkable orientation and concentration dependences of the electromechanical properties of $0.67Pb(Mg_{1/3}Nb_{2/3})O_3$–$0.33PbTiO_3$ single crystals. J Phys Condens Matter 16:2115–2128

Turik AV (1970) Elastic, piezoelectric, and dielectric properties of single crystals of $BaTiO_3$ with a laminar domain structure. Sov Phys Solid State 12:688

Vanderbilt D, Cohen MH (2001) Monoclinic and triclinic phases in higher-order Devonshire theory. Phys Rev B 63:094108

Voigt W (1910) Lerbuch der Kristallphysik. Teubner, Leipzig–Berlin

Ye ZG et al. (2001) Monoclinic phase in the relaxor-based piezoelectric/ferroelectric $Pb(Mg_{1/3}Nb_{2/3})O_3$–$PbTiO_3$ system. Phys Rev B 64:184114

Zembilgotov AG et al. (2005) Phase states of nanocrystalline ferroelectric ceramics and their dielectric properties. J Appl Phys 97:114315

Zhang R et al. (2003) Orientation dependence of piezoelectric properties of single domain $0.67Pb(Mn_{1/3}Nb_{2/3})O_3$–$0.33PbTiO_3$ crystals. Appl Phys Lett 82:3737–3739

Zheng H et al. (2004) Multiferroic $BaTiO_3$–$CoFe_2O_4$ nanostructures. Science 303:661–663